Discrete-time Reduced-complexity Youla Parameterization for Dual-input Single-output Systems

Xu Chen† and Masayoshi Tomizuka

Abstract— **A controller design is presented for directly shaping the sensitivity function in feedback control of dual-input single-output (DISO) systems. We provide special forms of discrete-time Youla-Kucera (YK) parameterization to obtain stabilizing controllers for DISO systems, and discuss concepts to achieve a reduced-complexity formulation. The proposed YK parameterization is based on an inverse of the loop transfer function, which gives benefits such as clearer design intuition and reduced complexity in construction. The algorithm is verified by simulations and experiments on hard disk drive systems, with application to wide-band vibration and harmonic disturbance rejections.**

Index Terms— **precision control, loop shaping, vibration rejection, discrete-time Youla parameterization, dual-stage actuation, dual-stage hard disk drives, multi-input single-output systems**

I. Introduction

Dual-stage actuation is a hardware solution to exceed the performance limit of single-actuator control systems. In this mechanical configuration, two actuators are combined for enhanced positioning: a coarse actuator with a long movement range, and a fine actuator, using e.g. piezoelectric materials, with a short stroke but a higher achievable accuracy. The fine actuator is mounted at the end of the coarse actuator to form a second-stage actuation, which commonly has enhanced mechanical performance at high frequencies, providing the capacity to greatly increase the servo bandwidth. Example applications of the technology include but are not limited to: hard disk drives (HDDs) [1], machine tools [2], [3], precision positioning tables and nanopositioners [4], [5].

In this study we investigate add-on loop-shaping designs via Youla parameterization for dual-stage systems. Youla parameterization [6], [7], aka Youla-Kucera (YK) parameterization and the parameterization for all stabilizing controllers, offers a parameterization of all stabilizing controllers, if a good model of the plant is available. Such a construction guarantees the closed-loop stability and renders loop shaping to simply the design of a stable Q filter. For single-input single-output (SISO) systems, YK parameterization has attracted lots of research attentions in controller tuning, adaptive control, and disturbance rejection [8]–[11]. Various challenges still exist for YK parameterization in dual-input single-output (DISO) systems. Reference [12] applied continuous-time multi-input multi-output (MIMO) YK formulations to the DISO system, and constructed the controller parameterization with two design filters Q and R. [12] also investigated the solvability of Q and R, and revealed the fundamental challenge of the two-degree-of-freedom design in standard YK parameterization. In [13], another standard state-space YK construction is adopted as a servo-enhancing element. Here, instead of a full DISO design, a SISO finite-impulse-response Q is used for the control of the secondary actuator.

We focus on the special class of DISO systems and discuss new investigations about YK parameterization for add-on feedback design. Add-on feedback refers to the design of additional features on a baseline control system. We show that for DISO [and more generally multi-input single-output (MISO) systems], we can formulate a reduced-complexity YK parameterization and obtain simpler realizations for loop shaping. Discrete-time YK design is known to have differences compared to the continuous-time version of the problem. A second contribution of this study is the development of a special DISO discrete-time coprime parameterization scheme, which makes the Q-filter design greatly simplified and approximately separated from the plant characteristics.

One challenging problem that suits for application of the proposed algorithm is the rejection of external vibrations in dual-stage HDD systems. Modern HDDs are applied to multimedia applications where servo control confronts much greater challenges than ever before. For instance, in all-in-one personal computers and digital TV accessories, HDDs are placed close to high-power speakers that generate a significant level of audio vibrations. Such external disturbances, after passing through the mechanical components, translate to structural vibrations of the HDD system, and excite relative movements between the read/write head and the track centers. Different from conventional narrow-band vibrations (e.g., internal disk flutters, fan noise) [14], audio vibrations are much more challenging to reject due to their intrinsic properties of having multiple resonances and very wide spectral peaks [15]. As the magnitudes of such external vibrations depend on the operation environment, flexible add-on servo design is

†: corresponding author. This work was supported by a research grant from Western Digital Corporation. Xu Chen is with the Department of Mechanical Engineering, University of Connecticut, Storrs, CT, 06269, USA (email: xchen@engr.uconn.edu). Masayoshi Tomizuka is with the Department of Mechanical Engineering, University of California, Berkeley, CA, 94720, USA (email: tomizuka@berkeley.edu)

essential for external-vibration rejection.

A short version of the results was presented in [16]. This study extends the results with full proofs of theorems, generalizations to broader systems, as well as full simulation and experimental results.

II. Standard YK Parameterization

Define $\mathcal{S}$ as the set of *stable, proper, and rational transfer functions*. For a SISO discrete-time system $P(z^{-1})$, YK parameterization starts with a coprime factorization of $P(z^{-1})$ to $N(z^{-1})/D(z^{-1})$, where $N(z^{-1})(\in \mathcal{S})$ and $D(z^{-1})(\in \mathcal{S})$ are coprime over $\mathcal{S}$, i.e., there exist $U(z^{-1})$ and $V(z^{-1})$ in $\mathcal{S}$ such that $U(z^{-1})N(z^{-1}) + V(z^{-1})D(z^{-1}) = 1$. If $P(z^{-1})$ can be stabilized by a negative-feedback controller $C(z^{-1}) = X(z^{-1})/Y(z^{-1})$, with $X(z^{-1})$ and $Y(z^{-1})$ being coprime factorizations of $C(z^{-1})$ over $\mathcal{S}$, then YK parameterization [6], [7] provides that any stabilizing feedback controller can be parameterized as

$$C_{all}(z^{-1}) = \frac{X(z^{-1}) + D(z^{-1})Q(z^{-1})}{Y(z^{-1}) - N(z^{-1})Q(z^{-1})},\ Q(z^{-1}) \in \mathcal{S} \qquad (1)$$

[1]Two important concepts are implied by the above result. First, a controller parameterized as (1) is guaranteed to generate a stable closed loop, as long as $Q(z^{-1})$ is stable. Second, any stabilizing controller can be realized in the form of (1).

A main benefit of (1) is that the closed-loop transfer functions become affine in $Q(z^{-1})$. Of particular interest is the sensitivity function (the closed-loop transfer function from the output disturbance to the plant output):

$$S(z^{-1}) = \frac{1}{1 + P(z^{-1})C_{all}(z^{-1})} \qquad (2)$$

$$= \frac{1}{1 + \frac{N(z^{-1})}{D(z^{-1})}\frac{X(z^{-1})}{Y(z^{-1})}}\left[1 - \frac{N(z^{-1})}{Y(z^{-1})}Q(z^{-1})\right] \qquad (3)$$

where $\left\{1 + [N(z^{-1})X(z^{-1})]/[D(z^{-1})Y(z^{-1})]\right\}^{-1}$ on the right side of (3) equals $S_o(z^{-1}) \triangleq 1/(1 + P(z^{-1})C(z^{-1}))$—the sensitivity function of the baseline closed loop consisting of $P(z^{-1})$ and $C(z^{-1})$.

For general MIMO systems, dimensions of transfer functions play important roles. Let $\mathcal{S}^{n_u \times n_y}$ denote the set of stable, proper, and rational transfer functions with n_u inputs and n_y outputs. Then:

Theorem 1: Consider an n_u-input n_y-output plant P. Let P be stabilized by a controller C (in a negative feedback loop), with $C = XY^{-1}$ ($X \in \mathcal{S}^{n_u \times n_y}$, $Y \in \mathcal{S}^{n_y \times n_y}$) and $P = ND^{-1}$ ($N \in \mathcal{S}^{n_y \times n_u}$, $D \in \mathcal{S}^{n_u \times n_u}$) being, respectively, right-coprime factorizations of C and P. Then the set of all stabilizing controllers for P is given by

$$\{(X + DQ)(Y - NQ)^{-1} :\ Q \in \mathcal{S}^{n_u \times n_y}\} \qquad (4)$$

or in the left-coprime format

$$\{(\bar{Y} - \bar{Q}\bar{N})^{-1}(\bar{X} + \bar{Q}\bar{D}) :\ \bar{Q} \in \mathcal{S}^{n_u \times n_y}\} \qquad (5)$$

[1]A mild condition that $Y(z=\infty) - N(z=\infty)Q(z=\infty) \neq 0$ is needed for the closed loop transfer functions to be proper and rational.

where $P = \bar{D}^{-1}\bar{N}$ ($\bar{N} \in \mathcal{S}^{n_y \times n_u}$, $\bar{D} \in \mathcal{S}^{n_y \times n_y}$) and $C = \bar{Y}^{-1}\bar{X}$ ($\bar{X} \in \mathcal{S}^{n_u \times n_y}$, $\bar{Y} \in \mathcal{S}^{n_u \times n_u}$) are, respectively, left-coprime factorizations of P and C.

For simplicity, we have omitted the index (z^{-1}) in the above theorem, and will adopt this format for long equations in the remaining analysis.

III. Proposed Algorithm for DISO Systems

Consider now the parameterization for dual-input single-output systems, with the general control structure shown in Fig. 1. Here $P(z^{-1}) = [P_1(z^{-1}),\ P_2(z^{-1})]$ is the DISO plant; $C(z^{-1}) = [C_1(z^{-1}), C_2(z^{-1})]^T$ is the single-input dual-output (SIDO) baseline controller.

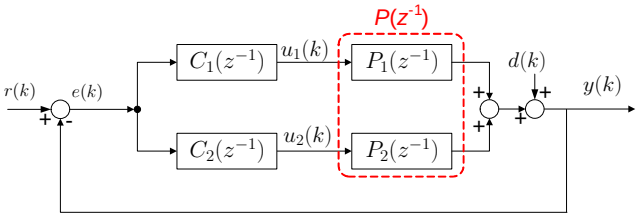

Fig. 1. General control structure for DISO systems

For this special class of MIMO system, the generalized (and more complicated) YK parameterization in Theorem 1 certainly works, however at the expense of reduced tuning intuitions and increased computation. More specifically, as $n_u = 2$ and $n_y = 1$ in Fig. 1, the Q parameter in both (4) and (5) will be a two-by-one SIDO transfer-function matrix. Compared to the SISO versions (1) and (3), both the controller and the sensitivity function will be more complex to implement and less intuitive to design.

A. Reduced-complexity formulation for DISO systems

To simplify the aforementioned difficulty, we discuss next a special YK parameterization for DISO systems. Notice that $P(z^{-1})$ is a dual-input system but the open-loop transfer function from $e(k)$ to $y(k)$ in Fig. 1 is always single-input single-output:

$$L(z^{-1}) = P_1(z^{-1})C_1(z^{-1}) + P_2(z^{-1})C_2(z^{-1}). \qquad (6)$$

If we treat $L(z^{-1})$ as a plant, then the baseline closed loop is composed of just two SISO elements: $L(z^{-1})$ and an identity feedback controller, as shown in Fig. 2.

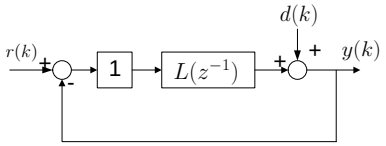

Fig. 2. SISO viewpoint of DISO feedback systems

We propose to perform YK parameterization for the fictitious plant $L(z^{-1})$. Consider a coprime factorization

$$L(z^{-1}) = N(z^{-1})/D(z^{-1}). \qquad (7)$$

For Fig. 2 we can choose $X(z^{-1}) = Y(z^{-1}) = 1$ for the identity feedback block, and obtain a simplified form of (1) for the DISO system:

$$\tilde{C}(z^{-1}) = \frac{1 + D(z^{-1})Q(z^{-1})}{1 - N(z^{-1})Q(z^{-1})},\ Q(z^{-1}) \in \mathcal{S}. \tag{8}$$

The controller in (8) can be realized by the dashed box in Fig. 3, which is an add-on scheme that can be switched on or off (by enabling or disabling the output of $Q(z^{-1})$), depending on the operation environments.

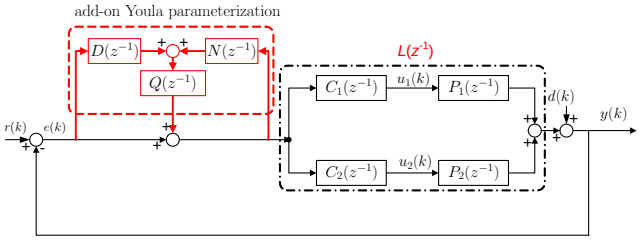

Fig. 3. Proposed YK parameterization for DISO systems

Theorem 2: Let $L(z^{-1}) = N(z^{-1})/D(z^{-1})$ be the coprime factorization of the fictitious plant in Fig. 3. Let the controller be designed as (8). Stability of the closed-loop system is guaranteed if $Q(z^{-1})$ is stable and the baseline feedback loop (without the add-on YK parameterization box) is stable. The closed-loop poles under (8) are composed of poles of the baseline feedback loop, and the poles of $Q(z^{-1})$, $N(z^{-1})$, and $D(z^{-1})$. Furthermore, the sensitivity function is

$$S(z^{-1}) = S_o(z^{-1})(1 - N(z^{-1})Q(z^{-1})) \tag{9}$$

where $S_o(z^{-1}) = 1/(1 + N(z^{-1})D^{-1}(z^{-1})) = 1/(1 + P(z^{-1})C(z^{-1}))$ is the baseline sensitivity function.

Proof: Let $N = \mathcal{B}_N/\mathcal{A}_N$, $D = \mathcal{B}_D/\mathcal{A}_D$, $Q = \mathcal{B}_Q/\mathcal{A}_Q$, where $\mathcal{B}_{\{\cdot\}}$ and $\mathcal{A}_{\{\cdot\}}$ denote, respectively, the numerator and the denominator of the transfer functions. Then based on (7) and (8),

$$L = \frac{N}{D} = \frac{\mathcal{B}_N\mathcal{A}_D}{\mathcal{A}_N\mathcal{B}_D},\ \tilde{C} = \frac{\mathcal{A}_D\mathcal{A}_Q\mathcal{A}_N + \mathcal{B}_D\mathcal{B}_Q\mathcal{A}_N}{\mathcal{A}_D\mathcal{A}_Q\mathcal{A}_N - \mathcal{A}_D\mathcal{B}_N\mathcal{B}_Q} \tag{10}$$

The closed-loop characteristic equation in Fig. 3 comes from

$$1 + L\tilde{C} = 0 \Leftrightarrow \mathcal{A}_D\mathcal{A}_Q\mathcal{A}_N(\mathcal{B}_N\mathcal{A}_D + \mathcal{B}_D\mathcal{A}_N) = 0 \tag{11}$$

where $\mathcal{B}_N\mathcal{A}_D + \mathcal{B}_D\mathcal{A}_N$ is the characteristic polynomial of the baseline feedback loop (obtained from $1 + L = 0$). The distribution of poles follows from (11).[2]

Finally, (9) is obtained by a substitution of $X(z^{-1}) = Y(z^{-1}) = 1$ to (3). ■

[2]Notice that the full order of the closed loop is the summation of the orders of L, D, N, and Q from Fig. 3. The *stable* poles from $\mathcal{A}_D$ and $\mathcal{A}_N$ are canceled between L and $\tilde{C}$ in (10). The output response will only reveal the dynamics of the poles from $\mathcal{A}_Q(\mathcal{B}_N\mathcal{A}_D + \mathcal{B}_D\mathcal{A}_N)$.

Design and implementation as an servo-enhancement scheme

From (9), the closed-loop sensitivity function is decomposed to the product of $S_o(z^{-1})$—the sensitivity function of the baseline system—and the Q parameterization term $1 - N(z^{-1})Q(z^{-1})$. This makes the proposed algorithm a tool for servo-enhancement design: after creating a baseline controller that provides basic feedback performance and robustness, add-on features can be directly introduced by designing $1 - N(z^{-1})Q(z^{-1})$, which is affine in the design parameter $Q(z^{-1})$. To reduce the gain of the new sensitivity function $S(z^{-1})$ (i.e., enhanced servo performance) in certain frequency region, we just need to design $N(z^{-1})Q(z^{-1})$ to approximate one in the same region. In addition, the baseline closed-loop poles are always reserved, and new poles (for different servo requirements) can be introduced by designing the stable $Q(z^{-1})$.

Remark: for designing $C_1(z^{-1})$ and $C_2(z^{-1})$ in Fig. 3, many tools are available, such as decoupled-sensitivity (see, e.g., [17]), PQ method [18], direct parallel design [19], and MIMO design methods such as LQG and H_∞/H_2 control (see [20] and the references therein). In this article, we focus on add-on servo enhancement, and refer interested readers to the aforementioned literature about design of the baseline feedback loop.

B. Coprime parameterization for the fictitious plant

One ideal case for (7) is that $N(z^{-1}) = 1$. This occurs if $L(z^{-1}) = 1/L^{-1}(z^{-1})$ is a valid coprime factorization, and will provide a beneficial result of $S(z^{-1}) = S_o(z^{-1})(1 - Q(z^{-1}))$, i.e., the Q design is completely separated from the dynamics of $L(z^{-1})$. If $L^{-1}(z^{-1})$ is not causal itself, the ideal factorization can be approximated by

$$L(z^{-1}) = z^{-m}/L_m^{-1}(z^{-1}) \triangleq z^{-m}[z^{-m}L^{-1}(z^{-1})]^{-1}. \tag{12}$$

Namely, we add delays so that $N(z^{-1}) = z^{-m}$, and that $D(z^{-1}) = z^{-m}L^{-1}(z^{-1})$ is proper/realizable.

The effect of delays: It is common for practical plants to have input delays. In a DISO setting, the proposed fictitious plant $L(z^{-1}) = P_1(z^{-1})C_1(z^{-1}) + P_2(z^{-1})C_2(z^{-1})$ has the advantage of reduced influence of delays. This is one main benefit compared to performing SISO YK parameterizations to $P_1(z^{-1})$ and $P_2(z^{-1})$ separately. Let $P_1(z^{-1}) = z^{-m_1}P_{1m}(z^{-1})$, $P_2(z^{-1}) = z^{-m_2}P_{2m}(z^{-1})$; and consider the example where $m_1 > m_2$. Without loss of generality, we assume that the controllers do not introduce additional separate steps of delays. Then $L(z^{-1}) = z^{-m_2}[z^{m_2-m_1}P_{1m}(z^{-1})C_1(z^{-1}) + P_{2m}(z^{-1})C_2(z^{-1})]$. For the term in the square bracket, the intermediate delay $z^{m_2-m_1}$ will be absorbed in the transfer function. The total delay for $L(z^{-1})$ is hence $m_2 = \min\{m_1, m_2\}$—the minimum of the delay steps among all actuators.

We now apply the concept of (12) to form an inverse-based coprime factorization of $L(z^{-1})$ for Fig. 3. If $L^{-1}(z^{-1})$ is stable, then $L(z^{-1}) = z^{-m}[z^{-m}L^{-1}(z^{-1})]^{-1}$ can be directly used. If not, we approximate it and form a

robust YK parameterization scheme. Denote $\hat{L}^{-1}(z^{-1})$ as the *nominal stable* inverse for $L(z^{-1})$. Notice that general feedback commonly aims at achieving a loop shape similar to that in Fig. 4. For such simple cases we can construct $\hat{L}^{-1}(z^{-1})$ by manually choosing poles and zeros to match the frequency response of $L(z^{-1})$. For a complex high-order stable $L(z^{-1})$, an optimal inverse design based on H_∞ minimization is provided in [21].

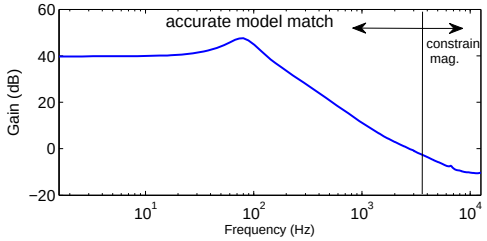

Fig. 4. General loop shape of $L(z^{-1})$ in servo design

C. The final implementation form and design intuitions

With the discussions in Section III-B, an approximate coprime factorization for $L(z^{-1})$ is

$$L(z^{-1}) = \frac{N(z^{-1})}{D(z^{-1})} \approx \frac{z^{-m}}{L_m^{-1}(z^{-1})} = \frac{z^{-m}}{z^{-m}\hat{L}^{-1}(z^{-1})} \tag{13}$$

and (9) becomes, in the frequency domain,

$$S(e^{-j\omega}) \approx S_o(e^{-j\omega})(1 - e^{-mj\omega}Q(e^{-j\omega})) \tag{14}$$

which is obtained by letting $z = e^{j\omega}$ and $\omega = 2\pi\Omega_{Hz}T_s$ (Ω_{Hz} is the frequency in Hz; T_s is the sampling time). At frequency ω, $S(e^{-j\omega})$ will have a small gain if $e^{-mj\omega}Q(e^{j\omega})$ is close to unity; if $|Q(e^{-j\omega})| \approx 0$ then $S(e^{-j\omega}) \approx S_o(e^{-j\omega})$, i.e., $S(e^{-j\omega})$ remains unchanged at frequencies where $|Q(e^{-j\omega})| \approx 0$.

Remark: Conventionally, the design of the Q filter in YK parameterization does not have a commonly agreed rule. General discrete-time YK parametrization usually applies an unstructured finite-impulse-response (FIR) filter [8]–[10]. In the continuous-time case, discussions on using a linear combination of some basis transfer functions [11], [22] have been explored. A more deeper cause of the diverse Q designs is perhaps the infinite choice of the plant parameterizations. Indeed, even for the general reduced-complexity design in (9), we would have $S(e^{-j\omega}) = S_o(e^{-j\omega})\left(1 - N(e^{-j\omega})Q(e^{-j\omega})\right)$. The Q-filter design hence is directly dependent on the desired servo performance as well as the frequency response of $N(z^{-1})$. The fundamental principle of Q design remains unchanged—in other words, to make $S(e^{-j\omega})$ small for enhanced servo at a particular frequency, $1 - N(e^{-j\omega})Q(e^{-j\omega})$ should be small; to keep the baseline performance at a frequency ω_o, $Q(e^{-j\omega_o})$ should be designed to approximate zero.

IV. Robustness Against Model Mismatch

This section considers the robustness of the proposed control scheme. Assume that the plant is perturbed to

$$\tilde{P}_i(z^{-1}) = P_i(z^{-1})(1 + W_i(z^{-1})\Delta_i(z^{-1})),\ i = 1,2 \tag{15}$$

with $|\Delta_i(e^{-j\omega})| \le 1\ \forall\omega$ and $W_i(z^{-1})$ being the uncertainty-weighting function. The overall feedback controller, consisting of the add-on YK control and the baseline $C_1(z^{-1})$ and $C_2(z^{-1})$ in Fig. 3, is given by

$$\bar{C}(z^{-1}) = \begin{bmatrix} \bar{C}_1(z^{-1}) \\ \bar{C}_2(z^{-1}) \end{bmatrix} = \frac{1 + D(z^{-1})Q(z^{-1})}{1 - N(z^{-1})Q(z^{-1})} \begin{bmatrix} C_1(z^{-1}) \\ C_2(z^{-1}) \end{bmatrix}. \tag{16}$$

Robust stability analysis in robust control theory seeks to find the minimum perturbation such that

$$\det\left(I + \tilde{P}(e^{-j\omega})\bar{C}(e^{-j\omega})\right) = 1 + \tilde{P}(e^{-j\omega})\bar{C}(e^{-j\omega}) = 0. \tag{17}$$

Theorem 3: For full perturbations where $\Delta_i(e^{-j\omega})$ can take any complex value satisfying $|\Delta_i(e^{-j\omega})| \le 1$, the proposed scheme is robustly stable if and only if nominal (i.e., when $W_i(e^{-j\omega}) = 0$) stability holds and

$$\frac{|P_1(e^{-j\omega})W_1(e^{-j\omega})\bar{C}_1(e^{-j\omega})| + |P_2(e^{-j\omega})W_2(e^{-j\omega})\bar{C}_2(e^{-j\omega})|}{|1 + P_1(e^{-j\omega})\bar{C}_1(e^{-j\omega}) + P_2(e^{-j\omega})\bar{C}_2(e^{-j\omega})|} < 1 \tag{18}$$

where $\bar{C}_i$ is from (16).

Proof: See Appendix A. ∎

Discussions: Certainly, there is always a tradeoff between performance and robustness. Despite the natural increase of stability requirement under heavy plant perturbations, from the performance viewpoint, the algorithm maintains the loop-shaping property for servo enhancement. To see this, let $L_{\text{pert}} \triangleq [\tilde{P}_1, \tilde{P}_2]\bar{C}$ be the perturbed loop transfer function and $\Delta = (P_1C_1W_1\Delta_1 + P_2C_2W_2\Delta_2)/(P_1C_1 + P_2C_2)$ be the normalized perturbation w.r.t. L. After substituting (15) and (16) in L_{pert} and separating the terms about $L = P_1C_1 + P_2C_2 = N/D$, the perturbed sensitivity function is

$$S_{\text{pert}} = \frac{1}{1 + L_{\text{pert}}} = \frac{1 - NQ}{1 + \frac{N}{D} + (1 + DQ)\frac{N}{D}\Delta} \tag{19}$$

where $1 - NQ$ is the term for the add-on performance enhancement. This effect does not change in the presence of plant uncertainties. .

For the term due to system uncertainty in (19), by controlling the magnitude of Q, we have the freedom to make $(1 + DQ)(N/D)\Delta$ small. As a special case, when $Q = 0$, (19) simplifies to the baseline perturbed sensitivity function $1/[1 + L(1 + \Delta)]$.

V. Generalization to SISO and MISO Systems

Recalling the proposed SISO viewpoint of loop shaping in Fig. 2, we observe that the block diagram is not limited to DISO plants where $L = P_1C_1 + P_2C_2$. For SISO and general MISO systems, the loop transfer function L obeys $L = \sum_{i=1}^{n_P} P_iC_i$ (n_P is the number of inputs). As long as the plant has only one output, the

loop transfer function L is always SISO and can be treated as the fictitious plant in Fig. 2. Results in the preceding analysis thus are directly applicable for SISO and general MISO systems.

For SISO plants with complex dynamics, one useful property of the proposed scheme is the capability of simplified factorization for L compared to P, as the general shape of L is relatively standard and can be approximated by low-frequency models (recall Fig. 4) while P can contain various complex dynamics.

VI. Q-filter Design, Simulation, and Experiments

With $S(e^{-j\omega}) \approx S_o(e^{-j\omega})(1-e^{-mj\omega}Q(e^{-j\omega}))$ in (14), loop-shaping design can simply concentrate on the add-on element $1-z^{-m}Q(z^{-1})$. This section provides two application examples in hard disk drive systems, one about repetitive tracking and regulation, another about rejecting disturbances including the audio vibrations described in Section I.

The simulation uses the dual-stage HDD benchmark system on Page 195 of [20]:

$$P_v(s) = \frac{2.04\times10^{21}}{s+3.14\times10^4}\,\frac{s^2+2073s+4.3\times10^8}{s^2+1508s+3.55\times10^8} \times \frac{1}{(s^2+301.6s+2.58\times10^5)(s^2+1244s+1.7\times10^9)}$$

$$P_m(s) = \frac{20\times5.45\times10^7}{s^2+2450s+1.7\times10^9}\,\frac{s^2+4524s+2.08\times10^9}{s^2+6032s+3.64\times10^9}$$

where the subscripts v and m denote, respectively, voice coil motor (VCM) and micro actuator (MA)—the main components of the two actuators. The plant models, whose magnitude responses are shown in Fig. 5, are obtained from an actual test drive system. The continuous-time models are sampled at a sampling time of $T_s = 0.04$ ms. The disturbance data is from actual measurements in audio-vibration tests on HDDs.

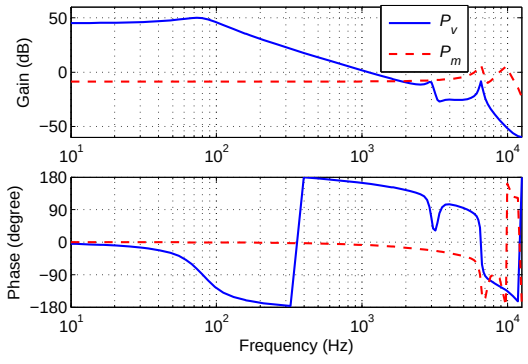

Fig. 5. Frequency responses of the plant

A set of notch filters are designed first to compensate the resonances:

$$N_v(z^{-1}) = \frac{1}{1.2356}\,\frac{z^2-1.416z+0.9415}{z^2-1.297z+0.92}\,\frac{z^2+0.1525z+0.95}{z^2+0.4155z+0.0144}$$

$$N_m(z^{-1}) = \frac{1}{2.0669}\,\frac{z^2+1.32z+0.7856}{z^2+0.6232z-0.277}\,\frac{z^2+0.148z+0.9}{z^2+0.439z+0.84}$$

The resonance-compensated plants are then treated as $P_1(=P_vN_v)$ and $P_2(=P_mN_m)$ for the model-based controller design. Using this approach, we simplify the nominal plant models to (see the verifications in Fig. 6)

$$\hat{P}_1(z^{-1}) = \frac{z^{-2}(0.0247+0.02444z^{-1}+0.00374z^{-2})}{1-2.272389z^{-1}+1.5540584z^{-2}-0.281376z^{-3}}$$

$$\hat{P}_2(z^{-1}) = 0.3674868z^{-1}$$

Notice that $\hat{P}_1(z^{-1})$ contains two steps of delays—less convenient for direct inverse-based SISO YK parameterization (recall Section III-B).

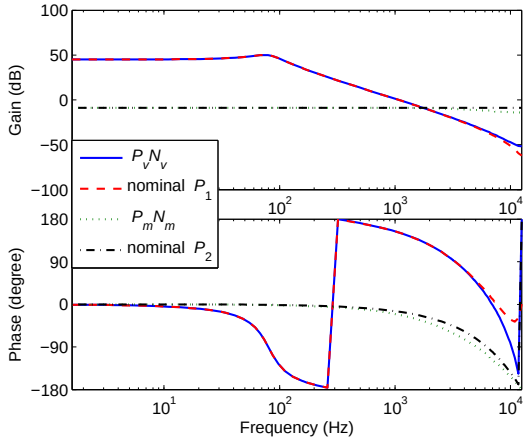

Fig. 6. Frequency responses of P_1, P_2, and their nominal models

The baseline controllers use the previously mentioned decoupled-sensitivity scheme, with $C_v(z^{-1}) = 1.6\times1.2356(1-0.9875z^{-1})^2/(1-0.2846z^{-1})/(1-0.99z^{-1})$, $C_2(z^{-1}) = 1.227\times2.0669(1-0.081z^{-1})/(1-0.9158z^{-1})$, and $C_1(z^{-1}) = C_v(z^{-1})(1+C_2(z^{-1})\hat{P}_2(z^{-1}))$. The design gives $1+L(z^{-1}) \approx (1+P_1(z^{-1})C_v(z^{-1}))(1+P_2(z^{-1})C_2(z^{-1}))$, so that $S_o(z^{-1}) = 1/(1+L(z^{-1})) \approx S_{1o}(z^{-1})S_{2o}(z^{-1})$ where $S_{1o}(z^{-1}) = 1/(1+P_1(z^{-1})C_v(z^{-1}))$ and $S_{2o}(z^{-1}) = 1/(1+P_2(z^{-1})C_2(z^{-1}))$ are respectively the decoupled sensitivities as if two independent feedback loops about $P_1(z^{-1})$ and $P_2(z^{-1})$ are formed. Fig. 7 shows the magnitude responses of the decoupled sensitivities, which corresponds to the example loop shape $L(z^{-1})$ previously shown in Fig. 4. The notch filtering and baseline design offer to provide a smooth magnitude response of $L(z^{-1})$. Hence although the order of $L(z^{-1})$ is 24, a low-order nominal $\hat{L}(z^{-1})$ can be readily obtained. By minimizing $\|L(z^{-1})-\hat{L}(z^{-1})\|_\infty$ with balanced model truncation via the square root method in MATLAB, a fourth-order $\hat{L}(z^{-1})$ is obtained. $N(z^{-1})$ and $D^{-1}(z^{-1})$ in (13) are, respectively, z^{-1} (i.e., $m=1$) and $L_m = 0.639743(1-0.9894z^{-1})(1-0.984z^{-1})(1-0.71196z^{-1})/[(1-0.99044z^{-1})(1-0.918129z^{-1})(1-1.987587z^{-1}+0.9879973z^{-2})]$, which is a minimum-phase system.

Combining the decoupled-sensitivity design and the proposed YK scheme, the new sensitivity function becomes [recall (14)], $S(z^{-1}) \approx S_{1o}(z^{-1})S_{2o}(z^{-1})(1-$

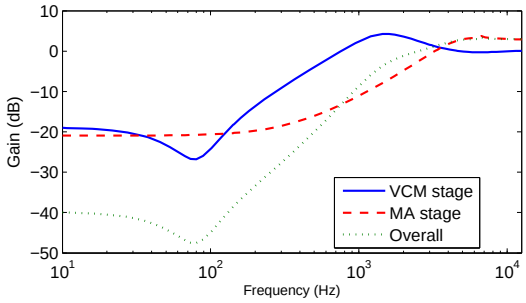

Fig. 7. Magnitude responses in the decoupled-sensitivity design

$z^{-m}Q(z^{-1})$)—the cascade of three independent components. With the form of $1-z^{-m}Q(z^{-1})$, the Q-filter design falls into the same class of problem as that in [21], [23]–[25].[3] For $m=1$, the following band-pass filter [21], [23]

$$Q(z^{-1}) = \frac{(\alpha-1)a + (\alpha^2-1)z^{-1}}{1 + a\alpha z^{-1} + \alpha^2 z^{-2}}, \tag{20}$$

or more generally, $Q(z^{-1}) = B_Q(z^{-1})/A_Q(z^{-1})$ with

$$A_Q(z^{-1}) = 1 + \sum_{i=1}^{n-1} a_i(\alpha^i z^{-i} + \alpha^{2n-i} z^{-2n+i}) + a_n \alpha^n z^{-n} + \alpha^{2n} z^{-2n}$$

$$B_Q(z^{-1}) = \sum_{i=1}^{2n} (\alpha^i - 1) a_i z^{-i+1}, \; a_i = a_{2n-i} \tag{21}$$

can achieve sample loop shapes as shown in Figs. 8 and 9 [n in (21) is the number of bands in the figures].

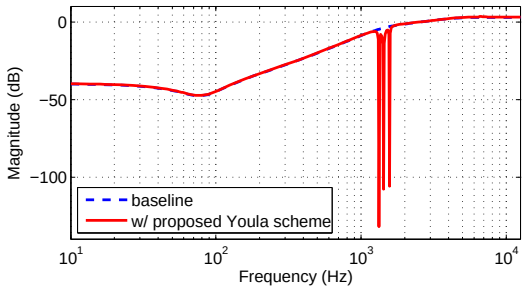

Fig. 8. Enhanced sensitivity functions for $n=3$ narrow bands

As the sensitivity function is the output disturbance rejection function, the reduced local gains in Fig. 8 make the design suitable for rejecting strong vibrations at several close frequencies. Fig. 9 expands the range of disturbance attenuation and suits for mixed structural vibrations that come from a frequency-rich excitation source. The change of notch width is controlled by the coefficient $\alpha \in (0,1)$ in (20) and (21). It can be observed that in both Figs. 8 and 9, $S(z^{-1})$ has very small gain at bands of frequencies, while amplifications

[3] [21], [23]–[25] discuss only SISO designs using the concept of extended disturbance observers. The Q-design methodology can however be applied to the problem in the present study.

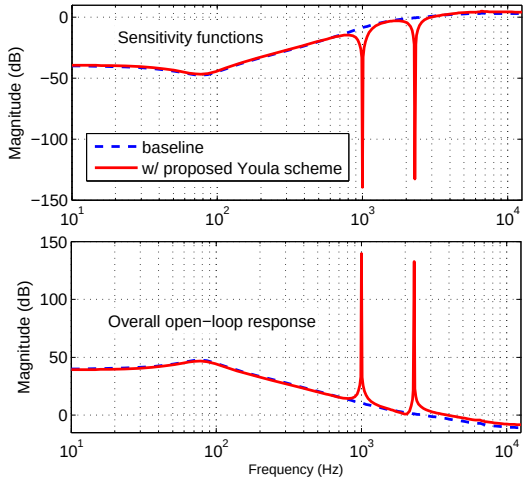

Fig. 9. Loop shaping design for rejection of two wide-band vibrations: upper plot—sensitivity functions $S_o(z^{-1})$ and $S(z^{-1})$; lower plot—corresponding open loop responses $L(z^{-1})$ and $L(z^{-1})\tilde{C}(z^{-1})$

at other frequencies are very small.[4] Fig. 9 also plots the magnitude response of the open-loop transfer function, which shows the equivalent effect of high-gain control at the disturbance frequencies.

Fig. 10 shows the error spectra under audio vibrations, with and without the design in Fig. 9. Due to the deep notches in the sensitivity function, the strong frequency components at around 1000 and 2300 Hz have been successfully rejected without visual amplification of other error components. Overall, the proposed algorithm provides an 42.3 percent of 3σ (σ is the standard deviation) reduction in the position error signal (PES).

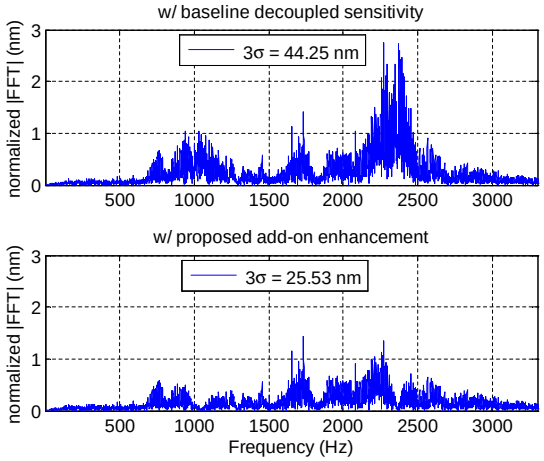

Fig. 10. Error spectra with and without compensation

[4] The coefficients a_i's in (20) and (21) determine the center frequencies of the notches in Figs. 8 and 9. For (20), we have $a = -2\cos(2\pi\Omega T_s)$, where Ω is the desired notch frequency in Hz. For the case with multiple bands, the filter parameter a_i in (21) and the notch frequency Ω_i satisfy $1 + \sum_{i=1}^{n-1} a_i(\alpha^i z^{-i} + \alpha^{2n-i} z^{-2n+i}) + a_n \alpha^n z^{-n} + \alpha^{2n} z^{-2n} = \prod_{i=1}^{n} (1 - 2\cos(2\pi\Omega_i T_s)\alpha z^{-1} + \alpha^2 z^{-2})$.

Fig. 11 compares the proposed design with the popular peak/resonant filter algorithm[5] [26], [27] for HDD band-limited disturbance rejection. Both algorithms are configured to achieve similar disturbance rejection at six wide frequency bands. Notice that the proposed algorithm focuses more on the overall target frequency range and has a larger effective attenuation range. The peak filter algorithm on the other hand is a combination of six "discrete" attenuation ranges, with less consideration on the overall performance (at some intermediate frequencies the disturbances are actually amplified). Another hidden difference is the capability of adaptive configurations. Interested readers can refer to [10], [21] for details of adaptive Q parameterization in YK schemes.

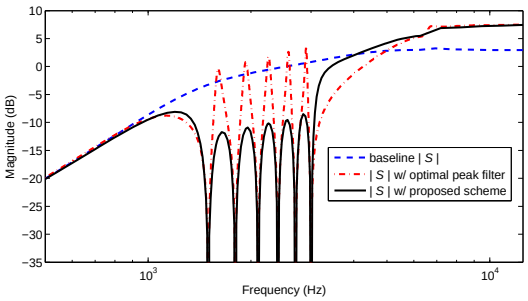

Fig. 11. Performance comparison with peak filter algorithm

The parameterization is additionally verified via experiments on a Western Digital 2.5-inch test drive, for rejection of repeatable runout (RRO) errors that come from nm-scale imperfections in the data tracks and disk rotations. Such errors are also typical in general mechanical systems involving periodic motions.

The Q-filter applies the enhanced repetitive control scheme recently developed in [25]: $Q(z^{-1}) = z^{-n_q} q(z,z^{-1})[(1-\alpha^N)z^{-(N-m-n_q)}]/[1-\alpha^N z^{-N}]$. Here, N is the period of the first harmonic component; $\alpha(\in[0,1])$ determines the width of attenuation region; $q(z,z^{-1})$ is a zero-phase low-pass filter for robustness; and n_q is the highest order of z in $q(z,z^{-1})$.

Fig. 12 shows the time trace of the PES and its FFT spectrum. In the illustrative example, $N = 310$, $m = 2$, $\alpha^N = 0.99$, and $n_q = 1$. The proposed algorithm is seen to effectively reject the harmonic disturbances in both time and frequency domains. In the top plot, the width of one track is in the order of 100 nm. In the bottom plot, it can be observed that the single Q filter compensates multiple spectral peaks in a large range of frequencies: nearly full rejection below 1000 Hz and partial rejection up to around 3000 Hz. Such attenuation is directly reflected in Fig. 13, which plots the magnitude response of $1-z^{-m}Q(z^{-1})$, i.e., changes in the sensitivity function due to the Q-filter design [recall (14)]. An additional 17

[5]The peak filter is added in the VCM stage; the baseline design uses the same decoupled-sensitivity loop shaping.

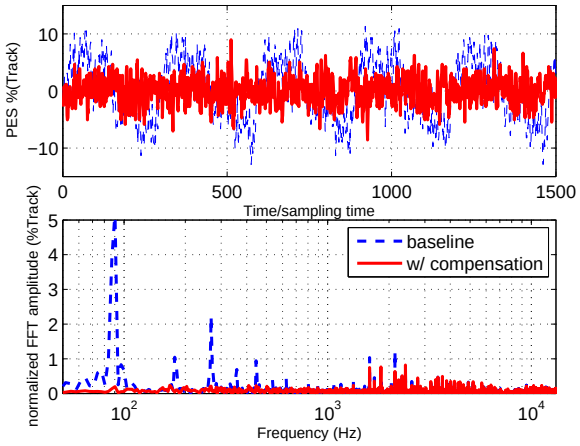

Fig. 12. Time-domain (top plot) and frequency-domain (bottom plot) disturbance rejection result for harmonic errors.

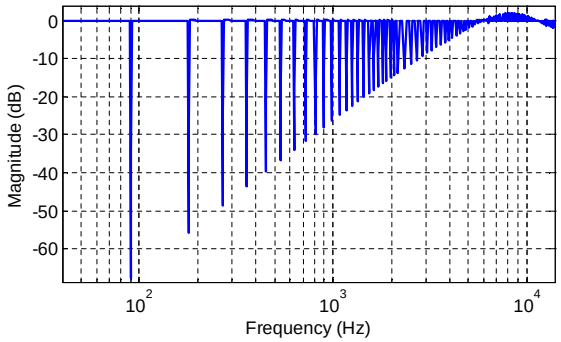

Fig. 13. Magnitude response of $1-z^{-m}Q(z^{-1})$ for RRO rejection

revolutions of data are collected and analyzed. The 3σ values of the error signal are shown in Table I. Here the baseline 3σ value is normalized to 100, and the proposed algorithm is seen to provide an overall 55.01 percent of performance improvement.

TABLE I

ALGORITHM PERFORMANCE IN REPEATABLE-ERROR REJECTION

	baseline	with proposed algorithm
Normalized 3σ	100	44.99

VII. CONCLUSION

We have introduced a loop-shaping concept for DISO systems (with extension to SISO and MISO systems). Mathematically, the proposed algorithm performs loop shaping via formulating the sensitivity function as $S \approx (1-NQ)/(1+P_1C_1+P_2C_2)$. Instead of directly augmenting the controllers C_1 and C_2, the idea of the proposed servo-enhancement design is to build a baseline system first and then focus on the affine add-on Q parameterization $1-NQ$. Several application examples have demonstrated the validity of the algorithm and explained its design intuitions. The loop-shaping idea is

seen, via both simulation and experiments, to provide strong flexibility in precision servos.

References

[1] D. Y. Abramovitch and G. F. Franklin, "A brief history of disk drive control," *IEEE Control Syst. Mag.*, vol. 22, no. 3, pp. 28–42, 2002.

[2] B.-S. Kim, J. Li, and T.-C. Tsao, "Two-parameter robust repetitive control with application to a novel dual-stage actuator for noncircular machining," *IEEE/ASME Trans. Mechatronics*, vol. 9, no. 4, pp. 644–652, 2004.

[3] W. Dong, J. Tang, and Y. ElDeeb, "Design of a linear-motion dual-stage actuation system for precision control," *Smart Materials and Structures*, vol. 18, no. 9, p. 095035, 2009.

[4] S.-K. Hung, E.-T. Hwu, M.-Y. Chen, and L.-C. Fu, "Dual-stage piezoelectric nano-positioner utilizing a range-extended optical fiber fabry-perot interferometer," *IEEE/ASME Trans. Mechatronics*, vol. 12, no. 3, pp. 291–298, 2007.

[5] C.-L. Chu and S.-H. Fan, "A novel long-travel piezoelectric-driven linear nanopositioning stage," *Precision Engineering*, vol. 30, no. 1, pp. 85 – 95, 2006.

[6] D. Youla, J. J. Bongiorno, and H. Jabr, "Modern wiener–hopf design of optimal controllers part i: The single-input-output case," *IEEE Trans. Autom. Control*, vol. 21, no. 1, pp. 3–13, 1976.

[7] V. Kucera, "Stability of discrete linear feedback systems," in *Proc. 6th IFAC World Congress, paper 44.1*, vol. 1, 1975.

[8] R. de Callafon and C. E. Kinney, "Robust estimation and adaptive controller tuning for variance minimization in servo systems," *Journal of Advanced Mechanical Design, Systems, and Manufacturing*, vol. 4, no. 1, pp. 130–142, 2010.

[9] F. B. Amara, P. T. Kabamba, and A. G. Ulsoy, "Adaptive sinusoidal disturbance rejection in linear discrete-time systems—part i: Theory," *Journal of Dynamic Systems, Measurement, and Control*, vol. 121, no. 4, pp. 648–654, 1999.

[10] I. D. Landau, A. C. Silva, T.-B. Airimitoaie, G. Buche, and M. Noe, "Benchmark on adaptive regulation–rejection of unknown/time-varying multiple narrow band disturbances," *European Journal of Control*, vol. 19, no. 4, pp. 237 – 252, 2013.

[11] B. D. Anderson, "From youla kucera to identification, adaptive and nonlinear control," *Automatica*, vol. 34, no. 12, pp. 1485 – 1506, 1998.

[12] J. Zheng, W. Su, and M. Fu, "Dual-stage actuator control design using a doubly coprime factorization approach," *IEEE/ASME Trans. Mechatronics*, vol. 15, no. 3, pp. 339–348, 2010.

[13] G. Guo, Q. Hao, and T.-S. Low, "A dual-stage control design for high track per inch hard disk drives," *IEEE Trans. Magn.*, vol. 37, no. 2, pp. 860–865, Mar. 2001.

[14] L. Guo and Y.-J. Chen, "Disk flutter and its impact on hdd servo performance," *IEEE Trans. Magn.*, vol. 37, no. 2, pp. 866 –870, Mar. 2001.

[15] J. R. Deller, J. H. L. Hansen, and J. G. Proakis, *Discrete-Time Processing of Speech Signals*. Wiley-IEEE Press, Sep. 1999.

[16] X. Chen and M. Tomizuka, "Reduced-complexity and robust youla parameterization for discrete-time dual-input-single-output systems," in *Proc. IEEE/ASME Int. Conf. on Adv. Intelligent Mechatronics, Wollongong, Australla, July 9-12*, 2013, pp. 490–497.

[17] R. Horowitz, Y. Li, K. Oldham, S. Kon, and X. Huang, "Dual-stage servo systems and vibration compensation in computer hard disk drives," *Control Engineering Practice*, vol. 15, no. 3, pp. 291–305, 2007.

[18] S. Schroeck, W. Messner, and R. McNab, "On compensator design for linear time-invariant dual-input single-output systems," *IEEE/ASME Trans. Mechatronics*, vol. 6, no. 1, pp. 50–57, Mar. 2001.

[19] T. Semba, T. Hirano, J. Hong, and L.-S. Fan, "Dual-stage servo controller for hdd using mems microactuator," *IEEE Trans. Magn.*, vol. 35, no. 5, pp. 2271–2273, Sep 1999.

[20] A. Al Mamun, G. Guo, and C. Bi, *Hard disk drive: mechatronics and control*. CRC Press, 2007.

[21] X. Chen and M. Tomizuka, "Selective model inversion and adaptive disturbance observer for time-varying vibration rejection on an active-suspension benchmark," *European J. of Control*, vol. 19, no. 4, pp. 300 – 312, 2013.

[22] J. C. Doyle, B. A. Francis, and A. Tannenbaum, *Feedback control theory*. Macmillan, 1992, vol. 134.

[23] X. Chen and M. Tomizuka, "A minimum parameter adaptive approach for rejecting multiple narrow-band disturbances with application to hard disk drives," *IEEE Trans. Control Syst. Technol.*, vol. 20, no. 2, pp. 408 –415, march 2012.

[24] X. Chen, A. Oshima, and M. Tomizuka, "Inverse based local loop shaping for vibration rejection in precision motion control," in *Proc. 6th IFAC Symposium on Mechatronic Systems, Hangzhou, China, April 10-12*, 2013, pp. 490–497.

[25] X. Chen and M. Tomizuka, "New repetitive control with improved steady-state performance and accelerated transient," *IEEE Trans. Control Syst. Technol.*, vol. 22, no. 2, pp. 664–675, March 2014.

[26] J. Zheng, G. Guo, Y. Wang, and W. Wong, "Optimal narrow-band disturbance filter for pzt-actuated head positioning control on a spinstand," *IEEE Trans. Magn.*, vol. 42, no. 11, pp. 3745–3751, 2006.

[27] T. Atsumi, A. Okuyama, and M. Kobayashi, "Track-following control using resonant filter in hard disk drives," *IEEE/ASME Transactions on Mechatronics*, vol. 12, no. 4, pp. 472–479, Aug 2007.

Appendix A: Proof of Theorem 3

Proof: Substituting (16) into (17) gives

$$1 + \tilde{P}_1(e^{-j\omega})\bar{C}_1(e^{-j\omega}) + \tilde{P}_2(e^{-j\omega})\bar{C}_2(e^{-j\omega}) = 0. \tag{22}$$

When nominal stability holds, the distance from $P(e^{-j\omega})\bar{C}(e^{-j\omega})$ to the $(-1,0)$ point is always positive, thus $1 + P_1(e^{-j\omega})\bar{C}_1(e^{-j\omega}) + P_2(e^{-j\omega})\bar{C}_2(e^{-j\omega}) \neq 0$. Dividing this quantity on both sides of (22) gives $[1 + \tilde{P}_1(e^{-j\omega})\bar{C}_1(e^{-j\omega}) + \tilde{P}_2(e^{-j\omega})\bar{C}_2(e^{-j\omega})]/[1 + P(e^{-j\omega})\bar{C}(e^{-j\omega})] = 0$. Substituting in (15) and using $P\bar{C} = P_1\bar{C}_1 + P_2\bar{C}_2$ yield $1 + P_1\bar{C}_1W_1\Delta_1/(1 + P\bar{C}) + P_2\bar{C}_2W_2\Delta_2/(1 + P\bar{C}) = 0$. The worst-case minimum perturbation happens when $|\Delta_1(e^{-j\omega})| = |\Delta_2(e^{-j\omega})| = |\Delta_o(e^{-j\omega})|$ and the perturbation directions are such that

$$1 - \left|\frac{P_1\bar{C}_1W_1}{1 + P\bar{C}}\right||\Delta_o| - \left|\frac{P_2\bar{C}_2W_2}{1 + P\bar{C}}\right||\Delta_o| = 0 \tag{23}$$

In other words, $|\Delta_o| = |1 + P_1\bar{C}_1 + P_2\bar{C}_2|/(|P_1\bar{C}_1W_1| + |P_2\bar{C}_2W_2|)$. If (18) is valid then $|\Delta_0| > 1$, which is not possible as $|\Delta_i| \leq 1$ by definition; hence the system is robustly stable. For the "only if" part of the proof, if (18) is violated, then $|\Delta_o| < 1$. Letting $|\Delta_1| = |\Delta_2| = |\Delta_o|$ with $\angle\Delta_i = -\angle\{P_i\bar{C}_iW_i/(1 + P\bar{C})\}$ achieves (23) and hence system instability. ■